

# Segmented MDI/HMDI-Based Polyurethanes with Lowered Flammability

Krzysztof Pielichowski,<sup>1</sup> Dominika Słotwińska,<sup>1</sup> Euzebiusz Dziwiński<sup>2</sup>

<sup>1</sup>Department of Chemistry and Technology of Polymers, Technical University, ul. Warszawska 24, 31-155 Kraków, Poland

<sup>2</sup>Institute of Heavy Organic Synthesis, ul. Energetyków 9, 47-225 Kedzierzyn-Kozle, Poland

Received 21 April 2003; accepted 14 July 2003

**ABSTRACT:** A series of segmented polyurethanes (PUs) based on 4,4'-diphenylmethane diisocyanate and 1,6-hexamethylenediisocyanate; polyoxypropylenediol (POPD); and low-molecular chain extenders, 1,2-propanediol or 3-chloro-1,2-propanediol was obtained by solution polymerization and characterized by GPC and microscopic methods. Spherical aggregates with diameter of about 200 nm, arranged in a quasi-linear mode, were observed by SEM technique; further investigations by the TEM method revealed hard-segment domains of longitudinal shape, with length of about 5–10 nm, showing some features of the arrangement along a “director” axis. The process of thermal decomposition was monitored by thermogravimetric analysis in both dynamic and isothermal mode; to gain a deeper look into the mechanism of decomposition, kinetic analysis was performed. First, isoconversional methods showed a multistep decomposition route, as the value of (apparent) energy of activation changes from about 150 kJ/mol in the first step up to about 350 kJ/mol in the third step, which corresponds to the

energy of dissociation of C—C bonds and leads to a char (carbonaceous) residue. Further calculations by means of the linear regression method revealed that kinetic model functions describing the degradation process of PU that does not contain chlorine were  $Bn_a \rightarrow An \rightarrow Fn$ , whereby for chlorine-containing polyurethanes the  $CnB \rightarrow An \rightarrow An$  model was applied as best fit. Volatile products were investigated by pyrolysis–gas chromatography/mass spectrometry method at 770°C; the low molecular weight decomposition products, which were identified, indicate that the depolymerization process, yielding mainly diols and isocyanates through breakage of urethane bonds, prevailed during the thermal treatment under pyrolytic conditions. Finally, the mechanism of thermal degradation of modified polyurethanes with lowered flammability was proposed. © 2004 Wiley Periodicals, Inc. *J Appl Polym Sci* 91: 3214–3224, 2004

**Key words:** polyurethanes; thermal properties; kinetics; pyrolysis; flame retardance

## INTRODUCTION

The thermal decomposition of polymers (their degradation attributed to absorbed thermal energy) constitutes an important phenomenon from both a fundamental and a technological perspective. Therefore, it is logical to analyze the decomposition process in such a way that both aspects are considered in a complementary fashion.

Fundamental research has established that the thermal decomposition of a polymeric material is a complex, heterogeneous process, consisting of several partial reactions.<sup>1</sup> The course of decomposition is affected by different factors, connected with the sample, with the degradation process alone, and with the surroundings determined by analytical equipment. A thermal analysis curve, which is the result of investigation by means of a thermal analysis method, depicts primary

and secondary reactions running during the decomposition process. A more complete analysis of the investigated phenomena is possible if methods for identification of volatile products are applied, such as the technique of pyrolysis–gas chromatography/mass spectrometry (Py-GC/MS).<sup>2</sup> A valuable tool toward a better understanding of degradation mechanisms of polymers offers methods for the evaluation of kinetic parameters, provided that the basic relationships and assumptions on which they are based are properly taken into account.

With respect to technological applications, the investigation of decomposition processes has a dual meaning. The first concerns stabilization of a polymer to obtain novel materials with a desired set of thermal properties/flame resistance that will be able to fulfill demands of contemporary material engineering.<sup>3</sup> The role and action of a stabilizer may be more effective, if a better understanding of polymer decomposition schemes is provided during its development. The stabilizers, including flame retardants, used so far were developed in a rather empirical fashion, but it seems that future generations of stabilizing systems will be obtained in a more deliberate way (i.e., using the

Correspondence to: K. Pielichowski (kpielich@usk.pk.edu.pl).

Contract grant sponsor: Polish State Committee for Scientific Research; contract grant number: 3 T09B 023 19.

knowledge arising from decomposition pathways). The second meaning of decomposition studies concentrates on the safe disposal or recycling of plastic wastes, which has become a social problem of growing importance nowadays. Both aspects are not contradictory, but rather complementary, particularly in the case of broadly used polymers such as polyurethane elastomers, which are a class of modern materials of commercial importance that are widely used (e.g., as automotive exterior body panels, medical implants, or flexible tubing).<sup>4-6</sup> They derive most of their useful properties from the incompatibility of the hard segments [e.g., 4,4'-diphenylmethane diisocyanate (MDI) extended with short-chain diols] and soft segments, which are usually composed of long-chain diols. Because the soft segments form a flexible matrix between the hard domains that in turn provide physical crosslinking, a complex, phase-segregated morphology can be observed that varies with the temperature.<sup>7,8</sup> At elevated temperature, the thermal stability of such a complex system is governed not necessarily by the weakest link in the chain but often by the environment, in that it has been shown that the polyester soft segment and the MDI/piperazine hard segment are more stable when mixed in the copolymer than when in separate phases.

The aim of this work was to investigate thermal properties of a series of segmented polyurethanes based on 4,4'-diphenylmethane diisocyanate; polyoxypropylenediol; and low molecular chain extenders, 1,2-propanediol or 3-chloro-1,2-propanediol. Polymers containing the latter low molecular chain extender have proved to be inherently flame-retardant materials.<sup>9</sup>

## EXPERIMENTAL

### Materials

For synthesis of segmented polyurethanes partially polymerized 4,4'-diphenylmethane diisocyanate (MDI, 31% of free isocyanate groups in relation to the pure MDI; Zchem Bydgoszcz, Poland) and 1,6-hexamethylenediisocyanate (HMDI; Aldrich, Steinheim, Germany), polyoxypropylene diol (POPD; Rokita S.A., Brzeg Dolny, Poland), 1,2-propanediol (PD; POCh, Gliwice,

TABLE I  
Description of Samples Used in This Study

Sample	Isocyanates content (%)		Diols content (%)		
	PMDI	HMDI	POPD	PD	CPD
1	90	10	60	40	0
2				30	10
3				20	20
4				10	30
5				0	40

TABLE II  
Molecular Weight and Polydispersity Coefficient of Samples 1-5

Sample	$M_n$ (g/mol)	$M_w$ (g/mol)	$M_w/M_n$
1	425	2312	4.87
2	411	2316	5.25
3	441	2287	5.56
4	409	2333	5.69
5	456	2724	5.97

Poland) or 3-chloro-1,2-propanediol (CPD; Aldrich), and 1-allyl-2-methylimidazole (catalyst; Zchem) were used. Ethyl acetate (POCh) was purified by distillation and used as a solvent during polymerization.

### Preparation

Segmented polyurethanes were prepared by a two-step (prepolymer) method, according to the following general procedure. In a thermostated reactor, isocyanate and polyoxypropylene glycol were reacted at 65°C for 2 h. The obtained prepolymer was dried under vacuum, and then subjected to further polymerization with a mixture of diols in the presence of catalyst (0.5 wt %). The reaction time was 30 min. MDI/sum of diols ratio was determined equivalently.

A detailed description of the synthesized samples is given in Table I.

### Techniques

#### Gel permeation chromatography (GPC)

Molecular weight was determined by GPC performed at 25°C on a Knauer 64 GPC System with a refractometric detector, with two PL-Gel Mixed-E columns. THF was used as the eluant at a flow rate of 0.8 cm<sup>3</sup> min<sup>-1</sup>, and the sample concentration was 5 mg cm<sup>-3</sup>. Polystyrene standards (Waters Chromatography Division/Millipore, Milford, MA) were used to construct a calibration curve. GPC data were processed using a CHROMA program to calculate average molecular weights,  $M_n$  and  $M_w$ , as well as polydispersity,  $M_w/M_n$ .

#### FTIR analysis

FTIR spectra were recorded on finely ground dispersions of PU samples in spectroscopic-grade KBr by using a Bio-Rad FTS 165 spectrometer (Bio-Rad, Hercules, CA), operating in the spectral range of 4000–400 cm<sup>-1</sup>.

#### Electron microscopy investigation

A scanning electron microscope (SEM, Philips XL30, The Netherlands) equipped with a detector of second-

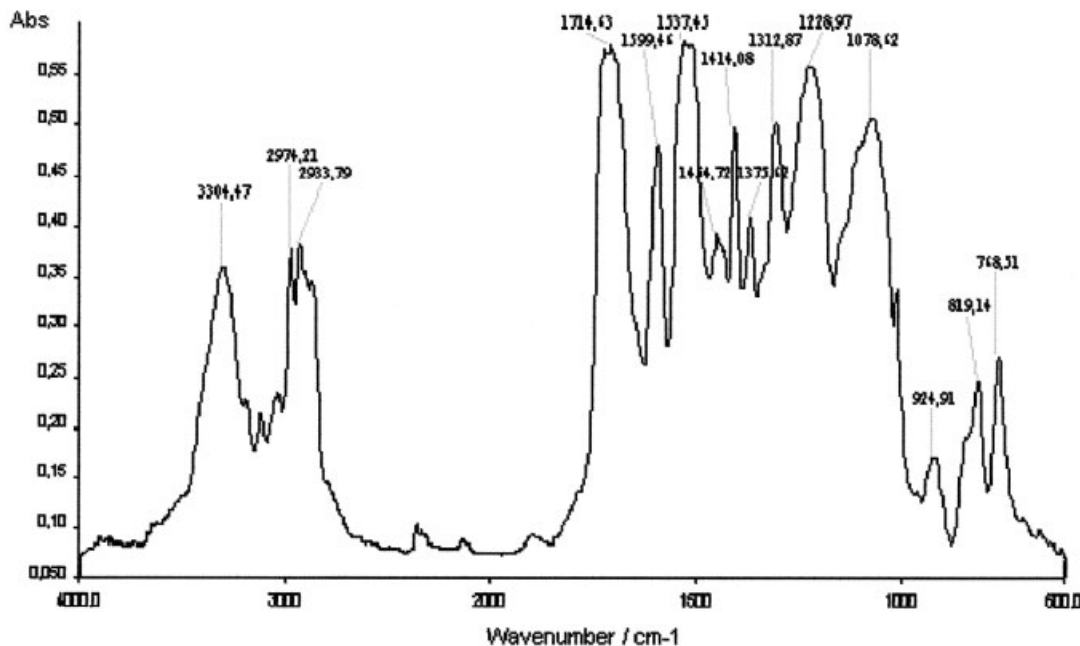


Figure 1 FTIR spectrum of sample 4.

ary electrons (SE), was used to investigate the surface morphology of gold-coated samples at an electron beam energy of 10 kV.

Transmission electron microscopy (TEM) measurements were performed using a Philips CM20 microscope at a voltage of 200 kV. Samples were in the form of thin films, placed on a Cu grid.

#### Thermogravimetric analysis (TG)

Thermogravimetric analysis was performed on a Netzsch TG 209 thermal analyzer, operating in a dynamic mode at a heating rate of 2.5, 5, 10, and 20 K/min or in an isothermal mode for 150 min. The conditions were as follows: sample weight, about 5 mg; atmosphere, argon; open  $\alpha$ -Al<sub>2</sub>O<sub>3</sub> pan. The raw

data were converted to ASCII files and kinetic analysis was carried out using an in-house program and a Netzsch Thermokinetic Program (v. 99/10) on an IBM-compatible computer with Pentium 4 processor.

#### Py-GC/MS

Flash pyrolysis experiments were performed using a Fischer 0316M pyrolyzer at 770°C coupled to the injector of a Hewlett-Packard 5890 Series II gas chromatograph (Hewlett-Packard, Palo Alto, CA). The gas chromatograph was programmed from 70 to 290°C at a rate of 7 K/min. Separation of the pyrolysis products was achieved using a fused-silica capillary column (30 m  $\times$  0.25 mm) coated with methylphenylsilicone phase ULTRA 2 (film thickness 0.25  $\mu$ m). Helium was used as the carrier gas at a flow rate of 1 mL/min. The compounds were

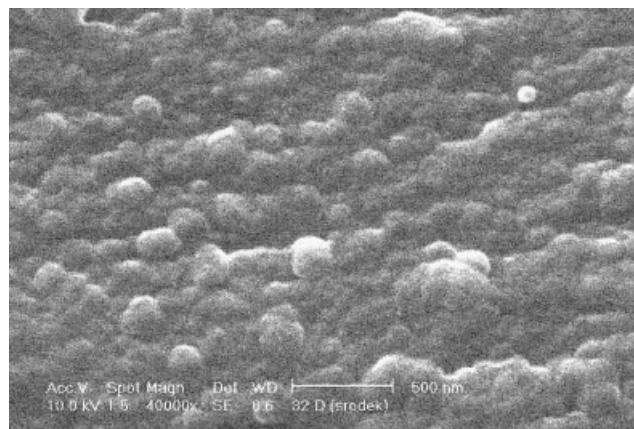


Figure 2 SEM microphotograph of sample 4 ( $\times 40,000$ ).

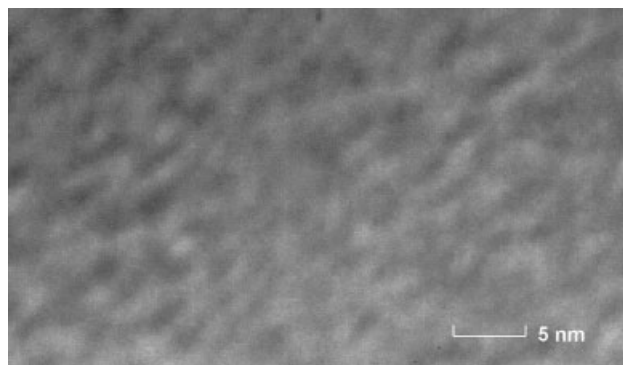


Figure 3 TEM microphotograph of sample 4 ( $\times 3.5 \times 10^6$ ).

TABLE III  
TGA Data of the Degradation Process of Samples 1–5 at 10 K/min Under Argon Atmosphere

Sample	IDT <sub>2%</sub> (°C)	T <sub>10%</sub> (°C)	T <sub>20%</sub> (°C)	T <sub>30%</sub> (°C)	T <sub>50%</sub> (°C)	Char residue (%)	DTG <sub>1 max</sub> (°C)	DTG <sub>2 max</sub> (°C)
1	86.4	157.2	273.9	317.1	361.9	26.3	227.1	353.7
2	84.6	154.6	281.2	323.1	378.2	26.8	287.2	360.3
3	82.8	153.7	282.9	322.1	365.0	26.7	287.1	354.6
4	119.2	210.6	290.6	318.9	369.6	27.8	292.6	354.1
5	130.9	230.0	287.8	308.2	358.9	22.2	292.1	353

detected using mass spectrometry under the following conditions: temperature of the transfer line GC/MS, 280°C; temperature of the ion source, 170°C; ionization energy, 70 eV; accelerating ions voltage, 1700 V; mass range, 14–550 amu.

## RESULTS AND DISCUSSION

Samples were characterized by GPC analysis, and results are collected in Table II.

The FTIR spectrum of sample 3, shown in Figure 1, confirms by characteristic absorption bands in the range 400–4000 cm<sup>-1</sup> [attributed to the following phenomena: 3315 cm<sup>-1</sup>, N—H stretching; 2980 cm<sup>-1</sup>, C—H stretching; 1718 cm<sup>-1</sup>, stretching oscillations in urethane, allophanate, and biuret groups (first amide band); 1598 cm<sup>-1</sup>, benzene ring skeleton oscillations and N—H def. in urethane group; 1524 cm<sup>-1</sup>, N—H def. in allophanate and biuret groups (second amide band); 1414 cm<sup>-1</sup>, C=O bond oscillations for hydrogen bond groups and allophanate and biuret groups; 1218 cm<sup>-1</sup>, asymmetric stretching oscillations in ether bond; 1073 cm<sup>-1</sup>, C—O—C stretching; and 767 cm<sup>-1</sup>,

N—H def.] the structural features of the TPU specimen used in this study.<sup>10</sup>

To reveal morphological features of the segmented polyurethanes, SEM measurements were made at 4 × 10<sup>4</sup> magnification (Fig. 2). It can be seen at this microstructural level that spherical aggregates, arranged in a quasi-linear mode, with diameter of about 200 nm occur.

More information about the microdomain structure can be obtained from TEM microphotographs, displayed in Figure 3. Hard-segment domains are of longitudinal shape, with length of about 5–10 nm; this dimension corresponds well with literature data, which give a value of 2.5–15 nm.<sup>11</sup>

Moreover, the structure shows some features of the arrangement along an axis (“director”); recently, some rod-coil diblock copolymers (and TPU can be regarded as being a segmented multiblock copolymer) were found to undergo a similar morphological behavior in which lamellar structures tend to arrange in a nematic ordering.<sup>12</sup>

On the other hand, the hard segments are preferentially locally oriented in a radial, rather than in a

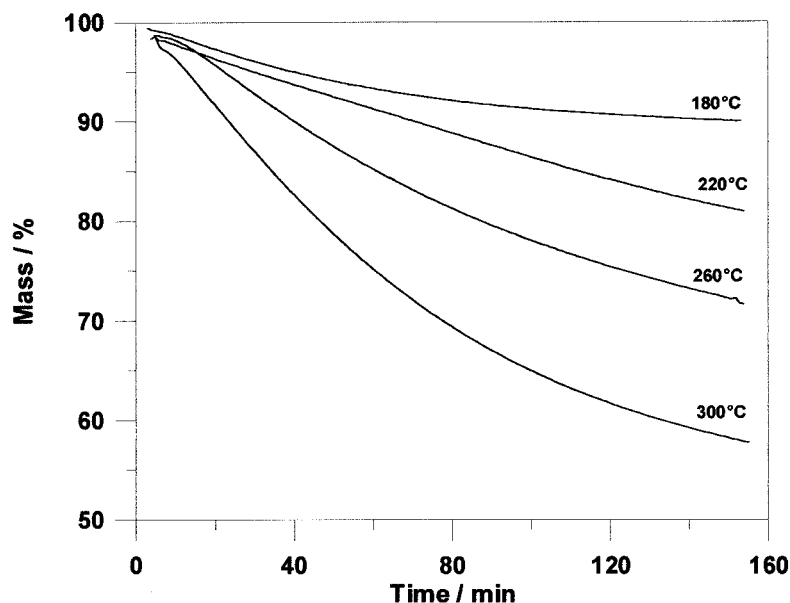


Figure 4 Isothermal TGA profiles of degradation of sample 4 ( $t_{\text{iso}} = 150$  min).

TABLE IV  
Kinetic Model Functions

Model	Symbol	$f(\alpha)$
Phase boundary-controlled reaction (contacting area)	R2	$(1 - \alpha)^{1/2}$
Phase boundary-controlled reaction (contracting volume)	R3	$(1 - \alpha)^{2/3}$
Random nucleation (Unimolecular decay law)	F1	$(1 - \alpha)$
Reaction $n$ th order	F $n$	$(1 - \alpha)^n$
Johnson-Mehl-Avrami	JMA	$n(1 - \alpha)[- \ln(1 - \alpha)]^{1-1/n}$
Two-dimensional growth of nuclei (Avrami equation)	A2	$2[- \ln(1 - \alpha)^{1/2}](1 - \alpha)$
Three-dimensional growth of nuclei (Avrami equation)	A3	$3[- \ln(1 - \alpha)^{2/3}](1 - \alpha)$
One-dimensional diffusion	D1	$1/2\alpha$
Two-dimensional diffusion	D2	$1/[- \ln(1 - \alpha)]$
Three-dimensional diffusion (Jander equation)	D3	$3(1 - \alpha)^{2/3}/2[1 - (1 - \alpha)^{1/3}]$
Three-dimensional diffusion (Ginstling-Brounshtein)	D4	$3/2[(1 - \alpha)^{-1/3} - 1]$
$n$ -Dimensional nucleation (Avrami-Erofeev equation)	An	$n[- \ln(1 - \alpha)^n](1 - \alpha)$
Reaction of 1st order with autocatalysis	C1	$(1 - \alpha)(1 + K_{\text{kat}}\alpha)$
Reaction of $n$ th order with autocatalysis	C $n$	$(1 - \alpha)^n(1 + K_{\text{kat}}\alpha)$
Prout-Tompkins equation	B $n$ a	$(1 - \alpha)^n\alpha^a$

tangential, arrangement.<sup>13</sup> The decomposition route is strongly affected by a pseudocrosslinking effect resulting from the hard-segment aggregation. The hard-segment domain generally exhibits a different degree of order or semicrystalline structure that was considered to be able to reinforce the hard-segment domain. Hence, the presence of an amorphous region may constitute the weakest part inside the hard-segment domain.<sup>14</sup>

It was previously postulated that the degree of phase separation plays a major role in the decomposition of polyurethanes.<sup>15</sup> Authors have investigated the thermal stability of two series of segmented poly(urethaneureas), containing three different kinds of polyether diols, and analyzed correlations with their soft-segment molecular weights and structures. The extent of interurethane hydrogen bonding, arising from the incomplete phase separation between the soft and hard segments, was found to influence the thermal stability of PUs under investigation. In another work,<sup>16</sup> an indirect evidence for the mutual stabilization effect of soft and hard phase was presented that is based on a protection function of soft segments through different functional groups.

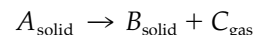
Considering the thermal properties of such a system, one should bear in mind that its thermal stability is limited not only by the energy of dissociation of the weakest link in the macrochain, but often by segmented microstructural morphology. Results of thermal investigations by the TGA method are displayed in Table III.

It can be seen that decomposition proceeds in three steps and the first derivative of the TG curve (DTG) displays two distinct maxima at 227–292°C and at about 360°C, whereby the char residue is in the 27% range.

Results of thermogravimetric analysis under isothermal conditions, displayed in Figure 4, show that

there are no thermal effects with “time of induction,” so that the thermal process can be further investigated by dynamic methods.

More information about the course of decomposition can be obtained on the basis of kinetic analysis; hence, our approach is based on the reaction expressed by the stoichiometric equation



The rate of reaction can be described in terms of two functions,  $k(T)$  and  $f(\alpha)$ ; thus

$$\frac{d\alpha}{dt} = k(T)f(\alpha) \quad (1)$$

where  $\alpha$  is the degree of conversion.

By substitution of the Arrhenius equation [ $k(T) = A \exp(-E/RT)$ ] the following equation may be obtained:

$$d\alpha/dt = A \exp(-E/RT)f(\alpha) \quad (2)$$

After introduction of the constant heating rate  $\beta = dT/dt$  and rearrangement, one obtains

$$\frac{d\alpha}{f(\alpha)} = \left(\frac{A}{\beta}\right) \exp\left(-\frac{E}{RT}\right) dT \quad (3)$$

where  $T$  is the temperature (K),  $f(\alpha)$  is the type of reaction,  $k(T)$  is the rate constant,  $E$  is the activation energy,  $A$  is the preexponential factor, and  $R$  is the gas constant.

A subsequent integration of eq. (3) leads to the equation

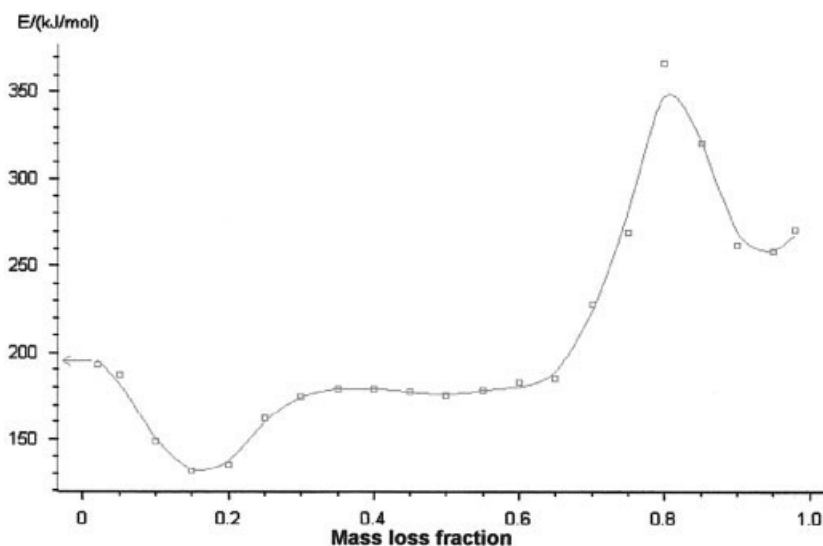


**Figure 5** Calculated values of the activation energy from the Ozawa–Flynn–Wall analysis of the degradation process of sample 4.

$$G(\alpha) = \int_0^\alpha \frac{d\alpha}{f(\alpha)} = \frac{A}{\beta} \int_{T_0}^T \exp\left(\frac{-E}{RT}\right) dT \quad (4)$$

which cannot be expressed by a simple analytical form because its right-hand side corresponds to a series of infinite  $\gamma$  functions. In mathematical practice logarithms are taken:

$$\ln G(\alpha) = \ln\left(\frac{AE}{R}\right) - \ln \beta + \ln p(x) \quad (5)$$

and the exponential integral  $p(x)$  is introduced:

$$p(x) = \frac{e^{-x}}{x} - \int_x^\infty \frac{e^{-x}}{x} dx \quad (6)$$

where  $x = E/RT$ .

Using an approximation of the exponential integral in a form proposed by Doyle<sup>17</sup>

$$\ln p(x) = -5.3305 + 1.052x \quad (7)$$

it is possible to determine the activation energy of the thermal process by following the specific heat flow of a process at several different heating rates:

$$\ln \beta = \ln\left(\frac{AE}{R}\right) - \ln G(\alpha) - 5.3305 + 1.052x \quad (8)$$

Equation (8) generates a straight line when  $\ln(\beta)$  is plotted against  $1/T$  for isoconversional fractions; the slope of the line is equal to  $-1.052E/R$  during a series of measurements with a heating rate of  $\beta_1 \cdots \beta_j$  at a

fixed degree of conversion of  $\alpha = \alpha_k$ . The temperatures  $T_{jk}$  are those at which the conversion  $\alpha_k$  is reached at a heating rate of  $\beta_j$ . This method was developed independently by Ozawa<sup>18</sup> and Flynn and Wall.<sup>19</sup>

Another isoconversional procedure, introduced by Friedman,<sup>20</sup> uses as its basis the following relationship:

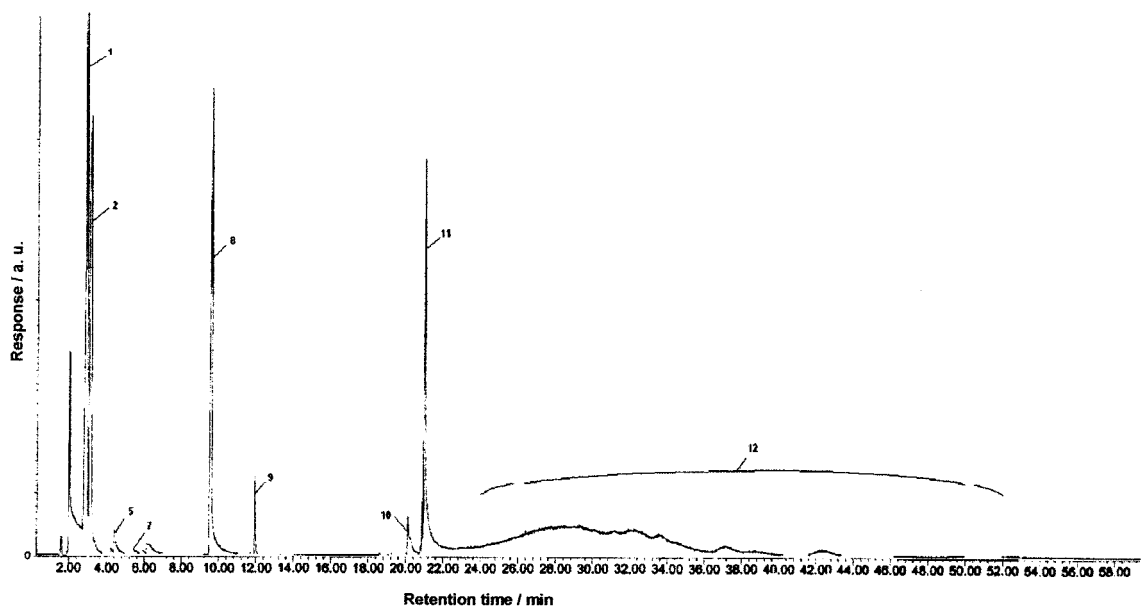
$$\ln\left(\frac{d\alpha}{dt}\right) = \ln f(\alpha) + \ln A - \frac{E}{RT} \quad (9)$$

which makes it possible to find the activation energy value from the slope of the line ( $m = -E/R$ ) when  $\ln(d\alpha/dt)$  is plotted against  $1/T$  for isoconversional fractions.

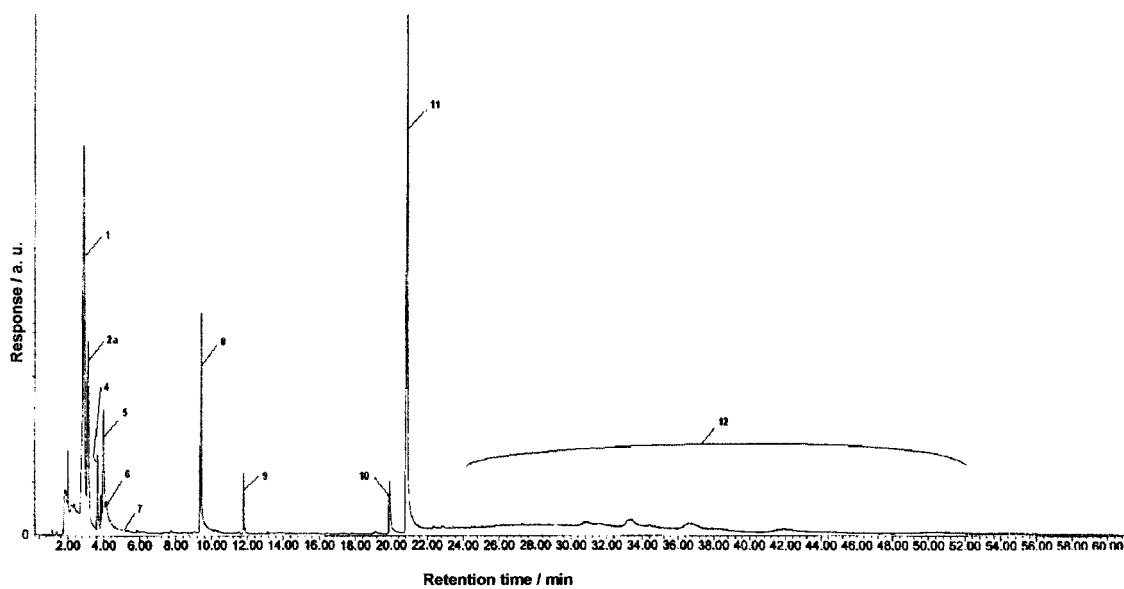
In eq. (1) the term  $f(\alpha)$  represents the mathematical expression of the kinetic model. The most frequently cited basic kinetic models are summarized in Table IV.

Nonisothermal curves of a thermal reaction can satisfy the kinetic equations developed for the kinetic analysis of “ $n$ th-order reactions,” even if they follow a quite different mechanism. Results of the comparative studies led to the conclusion that the actual mechanism of a thermal process cannot be discriminated from the kinetic analysis of a single TG trace.<sup>21</sup> Besides, both activation energy and preexponential factor, given in eq. (2), may be mutually correlated. As a consequence of this correlation any TG curve can be described by an apparent kinetic model instead of the appropriate one for a certain value of apparent activation energy. Therefore, the kinetic analysis of TG data cannot be successful unless the true value of the activation energy is known.<sup>22</sup>

Analysis of the changes of (apparent) energy of activation versus degree of conversion (Fig. 5) reveals



(a)



(b)

Figure 6 (a) Pyrogram of sample 1 at 770°C. (b) Pyrogram of sample 5 at 770°C.

that the process of thermal decomposition is a complex issue that cannot be analyzed by simple methods that assume a given  $f(\alpha)$  model (e.g., Kissinger<sup>23</sup> or Freeman-Carroll<sup>24</sup> methods).

At the first stage ( $0.1 < \alpha < 0.25$ ),  $E$  does not exceed 150 kJ/mol, which may be associated at this temperature range with the breakage of the urethane bond. It was previously observed that the heat liability of the urethane groups is dependent on the substituents in these groups.<sup>25</sup> The highest degradation temperature ( $\sim 250^\circ\text{C}$ ) was observed for urethane formed from alkyl isocyanate and alkyl alcohol, followed by an aryl

isocyanate-alkyl alcohol combination (degrading at  $\sim 200^\circ\text{C}$ ), an alkyl isocyanate and aryl alcohol (stable up to  $180^\circ\text{C}$ ), and an aryl-aryl combination whose temperature limit is in the  $120^\circ\text{C}$  range.

Then, for  $0.3 < \alpha < 0.65$  the energy of activation increases to about 180 kJ/mol, and, in the third step ( $\alpha > 0.7$ ) approaches nearly 350 kJ/mol, which corresponds to the energy of dissociation of C—C bonds, leading to a char (carbonaceous) residue.

The linear regression method was further used for calculation of the  $f(\alpha)$  function, from which it was found that  $f(\alpha)$  changes with the extent of decompo-

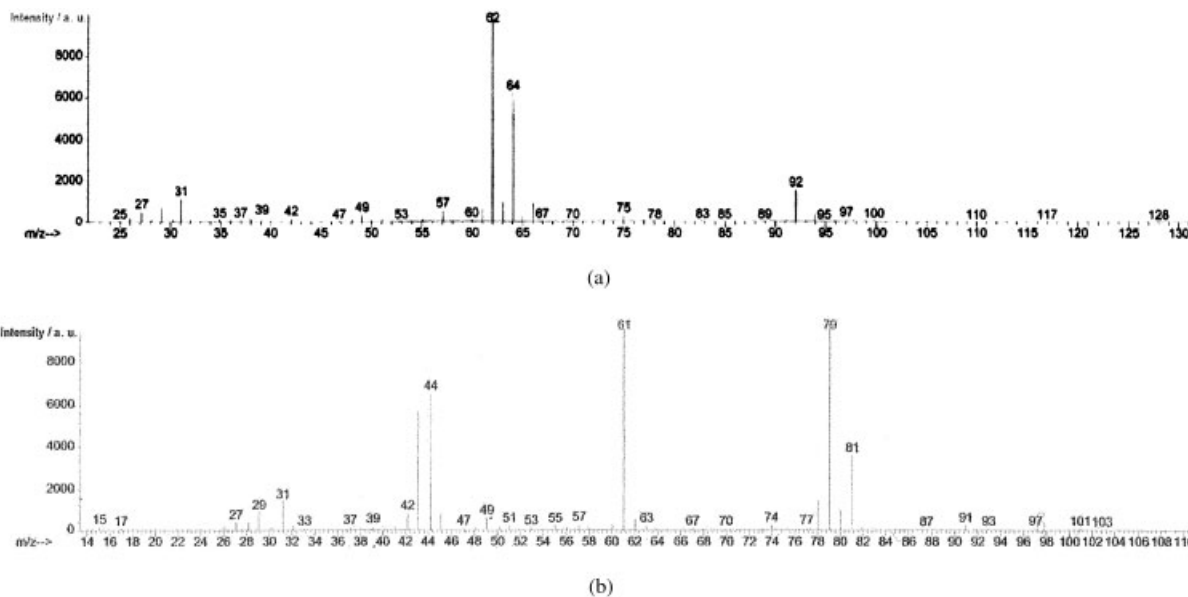


Figure 7 (a) Mass spectrum of component 4 obtained during pyrolysis of sample 5. (b) Mass spectrum of component 5 obtained during pyrolysis of sample 5.

sition; for PU that does not contain chlorine kinetic scheme  $Bn_a \rightarrow An \rightarrow Fn$  [where  $Bn_a$  represents the Prout-Tompkins equation;  $An$  represents an  $n$ -dimensional nucleation (Avrami-Erofeev equation);  $Fn$  represents an  $n$ th order reaction] was found, whereby for chlorine-containing polyurethanes  $CnB \rightarrow An \rightarrow An$  model was applied as best fit ( $CnB$ : reaction of  $n$ th order with autocatalysis). With respect to the kinetics of decomposition, the initial stage shows autocatalytic features that may have arisen from “irregular” struc-

tures, as previously observed for poly(vinyl chloride)<sup>26</sup> and polystyrene.<sup>27</sup>

Volatile products, investigated by Py-GC/MS and pyrograms of PU samples with or without 3-chloro-1,2-propanediol in the main chain are shown in Figure 6(a) and (b), respectively.

It may be seen that both pyrograms are similar to a certain extent given that both samples are based on the same type of diisocyanate. Differences occur for the retention times in the range of 3.8–7.0 min where for

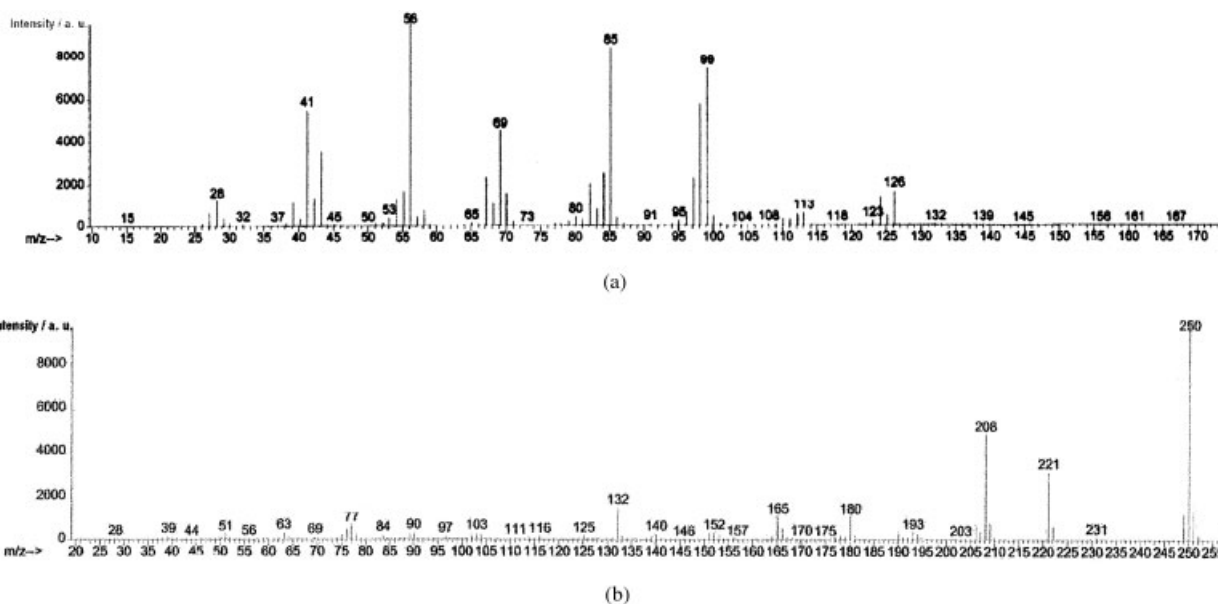
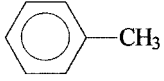
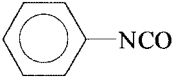
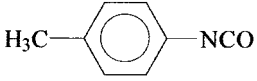
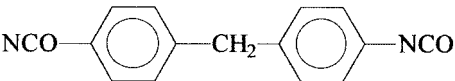


Figure 8 (a) Mass spectrum of component 8 obtained during pyrolysis of sample 5. (b) Mass spectrum of component 11 obtained during pyrolysis of sample 5.



TABLE V  
Identification of the Peaks of Figure 6(a) and (b) Assigned on the Basis of GC-MS and Library Searches

Peak	Chemical compound	Molar Mass (g/mol)	
1	Ethyl acetate	88	
2	$\begin{array}{c} \text{CH}_2\text{—CH}_2\text{—CH}_3 \\   \quad   \\ \text{OH} \quad \text{OH} \end{array}$	1,2-Propanediol	76
2		Toluene	92
3	$\begin{array}{c} \text{OH} \\   \\ \text{Cl—CH}_2\text{—CH—CH}_2\text{—Cl} \end{array}$	1,3-Dichloro-2-propanol	128
4	$\begin{array}{c} \text{Cl} \\   \\ \text{HO—CH}_2\text{—CH—CH}_2\text{—Cl} \end{array}$	2,3-Dichloro-1-propanol	128
5	$\begin{array}{c} \text{OH} \\   \\ \text{HO—CH}_2\text{—CH—CH}_2\text{—Cl} \end{array}$	3-Chloro-1,2-propanediol	110
6		Phenyl isocyanate	119
7		<i>p</i> -Methylphenyl isocyanate	133
8	NCO—(—CH <sub>2</sub> —) <sub>6</sub> —NCO	1,6-Diisocyanatohexane	168
9	4-Methyl-2,6-di- <i>tert</i> -butylphenol		220
10	MDI isomer		250
11		4,4'-Diphenylmethane diisocyanate	250
12	Propylene glycols		

sample 5 chloro-derivatives of propanol or propanediol were detected [Fig. 7(a) and (b)].

Major peaks marked as 8 and 11 in Figure 6(a) and (b) were identified as 1,6-hexamethylene-diisocyanate and 4,4'-diphenylmethane diisocyanate, respectively, [Fig. 8(a) and (b)].

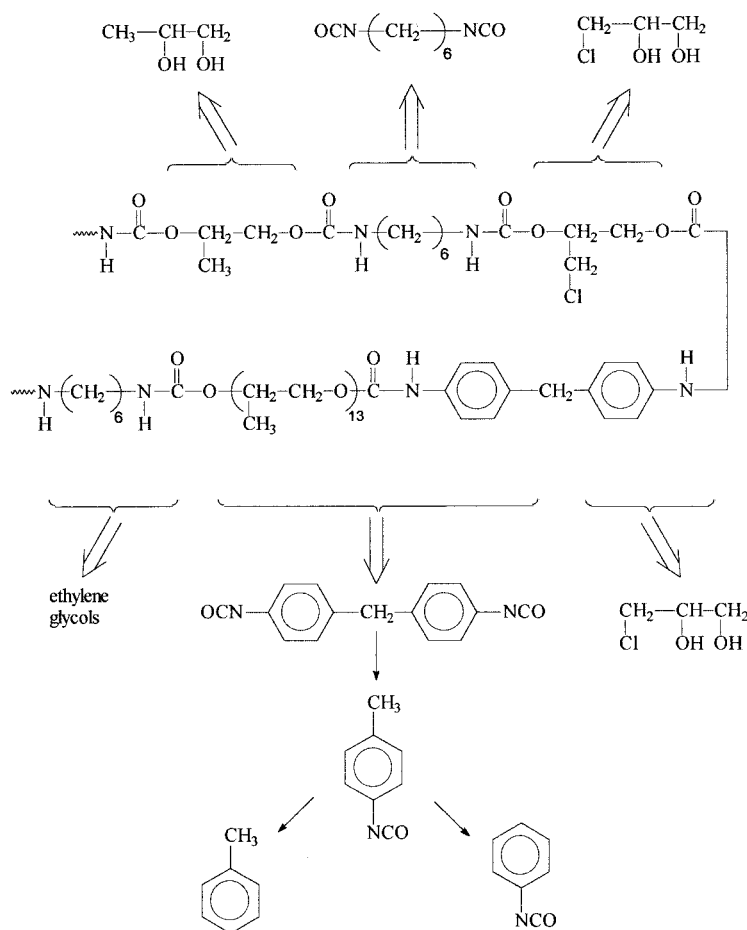
All major peaks were assigned to low molecular weight compounds, listed in Table V.

The detection of large amounts of monomers among the decomposition products indicates that depolymerization is the prevailing mechanism during pyrolysis of modified MDI/HMDI polyurethanes. Under rapid heating scission of urethane bonds occurred; however, the very low intensity of compounds 6 and 7 implies that pyrolysis of the polyurethane is most likely to occur by decomposition of the polyol section of the

structure; that is, breaking the bond between the RHN- and -COOR' groups leading to polypropylene glycol and other volatile species attributed to fragmentation of the polyether chain, plus the char residue observed in the "reaction zone" left on the sample surface after the pyrolysis experiment. A similar effect was observed during decomposition of rigid isocyanurate foams, studied by LP/TOFMS method.<sup>28</sup>

Chloro-derivatives that were detected are formed through intramolecular rearrangements of chloropropanediol; their stabilizing mode of action includes both gas-phase action and condensed-phase modification as found for the -Cl group on the benzene ring in epoxies or aromatic polyamides.<sup>29</sup>

The main directions of the decomposition under pyrolytic conditions are shown in Scheme 1.



**Scheme 1** Main directions of the samples' decomposition under pyrolytic conditions.

The obtained results yield additional information concerning the structure of polyurethanes under investigation: re-formation of monomers and small amounts of high molecular weight products (partially cured) indicate indirectly that, if the initial polymers show a moderate degree of crosslinking, it originates from van der Waals interactions rather than from chemical bonds in the form of allofanian and biuret structures.

## CONCLUSIONS

Segmented polyurethanes that contain chlorine in the hard segments proved to be thermally more stable than their nonmodified analogs: the greater the number of chlorine atoms located in the polymer structure, the higher the maximum temperature of the first derivative of the TG curve.

Kinetic analysis shows a complex behavior attributed to the changing value of the (apparent) energy of activation; kinetic model function exhibits both nucleation and chemical reaction features during the degradation process. Pyrolysis proceeds mainly through the depolymerization reaction, leading to the re-for-

mation of monomers and related compounds. Derivatives of the "reactive" flame retardant (3-chloro-1,2-propanediol), detected among decomposition products, seem to be active in both the gas and the condensed phase, thus influencing the overall decomposition rate. An interesting issue that remains to be explained concerns the influence of the microphase structure in multisegmental polyurethanes on their thermal stability and flammability; such studies are in currently in progress.

The authors are grateful to the Polish State Committee for Scientific Research for financial support (Grant 3 T09B 023 19).

## References

- Jellinek, H. H. G., Ed. *Degradation and Stabilization of Polymers*, Vol. II; Elsevier: Amsterdam, 1988.
- Blazsó, M. *J Anal Appl Pyrol* 1997, 39, 1.
- Pielichowski, K. *Polym J* 1997, 29, 848.
- Pielichowski, K.; Pielichowski, J.; Prociak, A. *J Appl Polym Sci* 1998, 67, 1465.
- Teo, L. S.; Chen, C. Y.; Kuo, J. F. *Macromolecules* 1997, 30, 1793.
- Velankar, S.; Cooper, S. L. *Macromolecules* 1998, 31, 9181.
- Wirpsza, Z. *Poliuretany: Chemia, Technologia, Zastosowanie*; WNT: Warsaw, 1991.

8. Słotwińska, D. Ph.D. Thesis, Cracow University of Technology, Poland, 2002.
9. Pielichowski, K.; Słotwińska, D. *Polym Degrad Stab* 2003, 80, 327.
10. Williams, D. H.; Fleming, J. *Spectroscopic Methods in Organic Chemistry*, IVth ed.; McGraw-Hill: London, 1987.
11. Oertel, G., Ed. *Polyurethane Handbook*; Hanser Publishers: Munich, 1994.
12. Woodward, A. E. *Understanding Polymer Morphology*; Hanser Publishers: Munich, 1995.
13. Wilkes, G. L.; Emerson, J. A. *J Appl Phys* 1976, 47, 4261.
14. Li, Y.; Gao, T.; Linliu, K.; Desper, C. R.; Chu, B. *Macromolecules* 1992, 25, 7365.
15. Wang, T. L.; Hsieh, T. H. *Polym Degrad Stab* 1997, 55, 95.
16. Ferguson, J.; Petrovic, Z. *Eur Polym J* 1976, 12, 177.
17. Doyle, C. D. *J Appl Polym Sci* 1962, 6, 639.
18. Ozawa, T. *Bull Chem Soc Jpn* 1965, 38, 1881.
19. Flynn, J. H.; Wall, L. A. *Polym Lett* 1966, 4, 232.
20. Friedman, H. L. *J Polym Sci* 1965, C6, 175.
21. Opfermann, J.; Kaisersberger, E. *Thermochim Acta* 1992, 203, 167.
22. Sestak, J. *Thermophysical Properties of Solids: Their Measurements and Theoretical Thermal Analysis*; Elsevier, Amsterdam, 1984.
23. Kissinger, H. E. *J Res Natl Bur Stand (US)* 1956, 57, 217.
24. Freeman, E. S.; Carroll, J. *Phys Chem* 1958, 62, 394.
25. Yang, W. P.; Macosko, C. W.; Wellinghoff, S. T. *Polymer* 1986, 27, 1235.
26. Starnes, W. M., Jr.; Girois, S. *Polymer Yearbook* 1995, 12, 105.
27. Audisio, G.; Bertini, F. *J Anal Appl Pyrol* 1992, 24, 61.
28. Price, D.; Gao, F.; Milnes, G. J.; Eling, B.; Lindsay, C. I.; McGrail, P. T. *Polym Degrad Stab* 1999, 64, 403.
29. Turi, E. A., Ed. *Thermal Characterization of Polymeric Materials*; Academic Press: San Diego, CA, 1997.